 CMES, vol.4, no.3&4, pp.489-496, 2003

Bone and Joints Modelling with Individualized Geometric and Mechanical Properties Derived from Medical Images

M.C. Ho Ba Tho[1]

Abstract: The objective of the paper is to address the methodology developed to model bone and joints with individualised geometric and material properties from medical image data. An atlas of mechanical properties of human bone has been investigated demonstrating individual differences. From these data, predictive relationships have been established between mechanical properties and quantitative data derived from measurements on medical images. Subsequently, geometric and numerical models of bones with individualised geometrical and mechanical properties have been developed from the same source of image data. The advantages of this modelling technique are its ability to study the 'patient' specificity. This should be of importance for quantifying bone and joint deformities and performing individualised preoperative planning surgery or orthopaedic treatment. In the same way, the efficiency of orthopaedic treatment with customised orthese or mechanical behaviour of implant in bone could be evaluated. Results would suggest improvement or development of new design.

keyword: Finite Element Model, Bone, mechanical properties, medical image.

1 Introduction

The paper will address the methodology we have developed in order to model bone and joints with appropriate geometric and mechanical properties derived from medical imaging. Medical imaging system such as MRI (Magnetic Resonance Imaging) CT (Computed Tomography) is commonly used to evaluate musculo-skeletal disease.

Numerical methods are used for solving physical and mechanical engineering problems. These numerical methods are appropriate for modelling such complex system as human bone and joints. Literature review demonstrated the extensive use of finite element modelling in biomechanics [Huiskes and Chao, 1983, Prendergast 1997, Vander Sloten et al. 1998]. According to our knowledge, the first two dimensional finite element model derived from medical image was obtained by digitising radiography [Carter et al. 1984], and three dimensional finite element model derived from digitised CT scans [HoBaTho et al. 1991, Fischer et al. 2003]. Then, extensive finite element models are obtained from CT data with most often a lack of description of the method allowing to model the geometry. One should note that few attention is given to the acquisition parameters and their consequences to the accuracy of bone modelling. Some author proposed specific protocol to optimise the reconstruction of a specific long bone (femur) from CT data (Viceconti et al. 1998) meanwhile other focus on the hardware and software parameters acquisition influence on the CT image assessment qualitatively and quantitatively (HoBaTho et Treutenaere 2001). Automatic FE generation have been developed using CT scans voxels [Keyak et al. 1990, 1993]. The voxels are converted directly in elements of equal size. Problems occurring with this technique are 1) their limitation in the accuracy of the model at the geometric and material boundaries and 2) the number of elements generated which would require specific algorithms of resolution. Besides these extensive numerical models, most of models are derived from CT data and few from MRI. Few consider appropriate material properties as they mostly are issued from literature (data or relationships). When experimental data do not confirm numerical simulation, material properties data are assessed experimentally by mechanical testing. This can only be performed on cadaveric specimen. As shown by the previous review, human bone has a non uniform geometry and a heterogeneous structure. One may expect differences from bone to bone and among individuals. In order to consider these intrinsic differences, it was necessary to develop a modelling technique describing appropriately and simultaneously the geometric and

[1] Université de Technologie de Compiègne (U.T.C.)
UMR CNRS 6600, Compiègne FRANCE

material properties. The methodology we have developed is based on a semi-automatic generation of a three dimensional geometric model of bone and joints anatomy derived from medical imaging CT or MRI data. Predictive relationships obtained from previous work demonstrated significant correlation between the material properties and quantitative measurements derived from imaging techniques [Rho et al. 1995]. Then, from the same source of medical imaging data, numerical models with individualised geometric and mechanical properties were developed.

2 Methods

2.1 Assessment of geometry via medical imaging techniques

There are different modalities of medical imaging techniques to explore bone and joints: X-ray radiographs, CT scanner (Computed Tomography), MRI (Magnetic Resonance Imaging). The two first techniques are based on absorption of X-rays, and are often used to diagnose bone disease. Meanwhile the last one is based on proton resonance and is more dedicated to soft tissue such as ligaments, cartilage besides bone structures are also visualised.

In order to assess the anatomical data, we have developed a pre processing medical image CT and MRI [SIP 305, ©Inserm, HoBaTho 1993].

The different steps of the image processing were 1) to decode the stack of medical image data representing the three dimensional of bone and joints structure, 2) to perform an edge detection after a threshold process and 3) to build geometric entities of the bones with a creation of an output data file in a neutral format or an IGES format.

2.1.1 Medical Image Processing

The standard exchange format file of the medical image derived from ACR-NEMA[2] specifications is DICOM[3]. Once the medical images are decoded, image processing can be performed. A pixel is coded on 12 bits i.e. pixel values varies from 0 (white) to 4096 (black). The next step was to perform the threshold process. It consists in giving threshold values based on the histogram representing the distribution of pixel values. As a result only anatomical contours of interest are visualised on the binary image (only two levels 0 and 1, white and black). Then segmentation by region was used, the edge detection allowed the outlines of the anatomical structure to be obtained. The edge detection consists in Hermite parametric cubic curves interpolation. Their formulation is obtained from a parametric cubic equation (Eq.1) and geometric constraints on two ending points.

$$P(u) = [x(u), y(u), z(u)]$$
$$P(u) = \sum_{k=0}^{3} a_k u^k \qquad u \in [0,1] \tag{1}$$

Their final expression form with blending functions are expressed in Eq.2.

$$P(u) = P_0(1-3u^2+2u^3) + P_1(3u^2-2u^3) + P_0'(u-2u^2+u^3) + P_1'(-u^2+u^3) \tag{2}$$

P_0, P_1, P_0', P_1': ending points and associated derivatives.

The geometric continuity of two curves is obtained by defining same tangent at the ending points of the first curve and the first point of the second curve as illustrated in Fig 1. Surfaces connecting these curves were Hermite

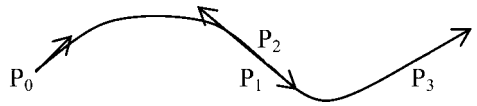

Figure 1 : Hermite parametric cubic curves

bicubic polynomials defined by Eq.3.

$$P(u) = \sum_{i=0}^{3}\sum_{j=0}^{3} a_{ij} u^i v^j \qquad u,v \in [0,1] \tag{3}$$

The different steps of a three dimensional geometrical reconstruction *in vivo* of human long bone (tibia) from CT data is illustrated in Fig. 2. The pre and post processor Patran (MSC.Software) is used for the visualisation of the geometric entities written in a neutral file (see Fig.3).

Once the geometrical data was obtained, finite element meshing was performed via any commercial software.

[2] American College of Radiology and National Electric Manufacturers Association

[3] Digital Imaging COmmunication in Medicine

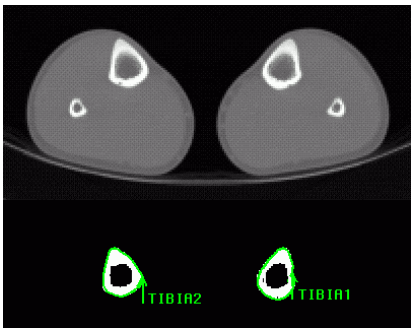

Figure 2 : Edge detection of a transverse CT slice after the threshold process.

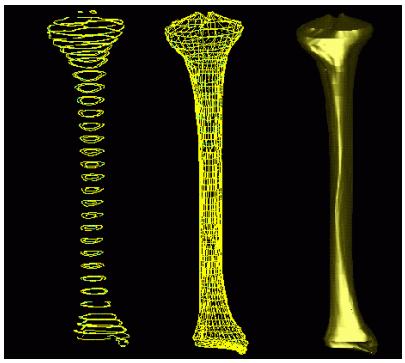

Figure 3 : Three dimensional geometrical reconstruction of bone contours (lines and surfaces).

In order to model realistic bone anatomy, it is necessary to associate the appropriate mechanical properties of the bone.

2.2 Mechanical properties of human bone

Mechanical properties of bone have been studied for over three decades in order to understand the mechanical behaviour of bone in the process of fracture risk, repair and bone related disease. Besides, few data were available or insufficient for human bone modelling. Human bone is highly heterogeneous and anisotropic material. It can be compared to composite materials; it is made of two different tissue spongious bone (high porosity) and cortical bone (compact bone) depending on the anatomical location. Bone was assumed to have an orthotropic behaviour which stiffness matrix containing elastic constants were defined by Eq 4. By reversing the stiffness matrix, the compliance matrix allowed the elastic properties in the three axes of symmetry of the crystal to be determined (Eq. 5.).

$$[C_{ij}] = \begin{bmatrix} C_{11} & C_{12} & C_{13} & 0 & 0 & 0 \\ C_{21} & C_{22} & C_{23} & 0 & 0 & 0 \\ C_{31} & C_{32} & C_{33} & 0 & 0 & 0 \\ 0 & 0 & 0 & C_{44} & 0 & 0 \\ 0 & 0 & 0 & 0 & C_{55} & 0 \\ 0 & 0 & 0 & 0 & 0 & C_{66} \end{bmatrix} \quad (4)$$

$$[S_{ij}] = \begin{bmatrix} \frac{1}{E_1} & -\frac{\nu_{21}}{E_2} & -\frac{\nu_{31}}{E_3} & 0 & 0 & 0 \\ -\frac{\nu_{12}}{E_1} & \frac{1}{E_2} & -\frac{\nu_{32}}{E_3} & 0 & 0 & \\ -\frac{\nu_{13}}{E_1} & \frac{\nu_{23}}{E_2} & \frac{1}{E_3} & 0 & 0 & 0 \\ 0 & 0 & 0 & \frac{1}{G_{23}} & 0 & 0 \\ 0 & 0 & 0 & 0 & \frac{1}{G_{31}} & 0 \\ 0 & 0 & 0 & 0 & 0 & \frac{1}{G_{12}} \end{bmatrix} \quad (5)$$

E_i : Young's moduli in the direction i,
G_{ij} : Shear moduli in plane i-j
ν_{ij} : Poisson's ratio stress and strain respectively in directions i,j.

Experimentally, we used an ultrasonic transmission technique for assessing bone material properties. Different wave propagation techniques were used for velocities measurements of bone tissue. Bulk velocities were measured for cortical bone, and then elastic constants were obtained. Cancellous bone is porous and highly heterogeneous compared to cortical bone. Homogeneous volume needed to be assumed and bar waves were used, allowing to assess directly the elastic properties [Ashman et al. 1984, 1989]. Then, an atlas of mechanical properties has been performed in order to obtain a database of material properties of different types of bone (femur, tibia, mandible, humerus, patella, lumbar spine) from eight unembalmed subjects (7 males, 1 female, mean age 60 years (45-68)) [HoBaTho et al. 1992, HoBaTho et al. 1998].

Typical range of values of mechanical properties for cortical bone and cancellous bone are summarised in Table 1 [HoBaTho et al. 1991].

2.3 Models with individualised geometric and material properties from CT data.

In order to associate geometric and mechanical properties, we assume that measurements derived from medical imaging could predict material properties. We have investigated the relationships between CT number derived from CT imaging technique and mechanical properties of bone. The CT number characterize a linear coefficient of

Table 1 : Range of values of mechanical properties obtained from eight subjects. Minimum, maximum and median values are given.

Bone	cortical	cancellous
E_{axial}(GPa)	14 -27 20	0.011-3.12 0.961
$E_{tangential}$(GPa)	7-17 12	0.023 -1.5 0.341
E_{radial}(GPa)	7-16 11	0.024-1.5 0.301
ρ(kg/m^3)	1545-2118 1840	55-744 257
CT (HU)	1270-1835 1560	-72-512 143
σ_{ult} (MPa)	* 	0.11-11 3

* Ultimate strength of cortical specimen were not measured, literature review gave typically values around 150MPa.

Table 2 : Predictive relationships for the proximal tibia. Young's modulus is expressed in MPa and density in kg/m^3 and CT number in HU.

Relationships	
$E_{axial} = 0.51\rho^{1.37}$	$R^2 = 0.96$
$E_{tangential} = 0.06\rho^{1.55}$	$R^2 = 0.90$
$E_{radial} = 0.06\rho^{1.51}$	$R^2 = 0.89$
$E_{axial} = 296 + 5.2CT$	$R^2 = 0.79$
$\rho = 114 + 0.916CT$	$R^2 = 0.80$

attenuation of X-ray within the tissue. For the CT scan, the pixels values are represented by an empirical number called CT number expressed in Houndsfield Units (HU) and is defined by the following empirical equation:

$$CT(HU) = 1000\frac{CT - CT_{water}}{CT_{water} - CT_{air}} \tag{6}$$

$$CT(HU) = 1000\frac{\mu - \mu_{water}}{\mu_{water} - \mu_{air}} \tag{7}$$

μ is the linear coefficient of attenuation of X-ray within the tissue (cm^{-1}). CT number value is depending on acquisitions parameters, typical values are 0 and –1000 for water and air respectively.

Table 2 summarised some predictive relationships between elastic properties and density and CT numbers (Rho et al. 1995) of the proximal tibia (upper extremity of the tibia).

From the same source of images data, a geometric reconstruction was performed as described previously and a finite element model was then performed via a commercial software. A custom made program mesh matching properties has been developed allowing the matching of the material properties distribution measured on the stack of CT image data and their assignment to the elements properties. The program consists in matching the measured mean CT number of a region of interest (ROI) with the characteristics geometric properties of the elements of the mesh. It should be noted that for the three dimensional mesh, it is necessary to match the technical acquisition parameters of the CT data with that of the protocol used to get the predictive relationships and the three-dimensional mesh.

3 Applications

3.1 Modelling of bone and joints of children

The clinical application of the developed methods is to evaluate bone and joint disease in children (congenital dislocation of the hip (hip deformity) [Roach et al. 1997], clubfoot (foot deformity) [Johnston et al. 1995], rotational abnormalities of the lower limbs [Limbert et al. 1998, Périé et HoBaTho 1998], scoliosis (spine deformity) [Périé et al. 2001]. Geometric model of the knee from MRI, allowed to perform kinematic analysis in vivo and quantification of contact areas using a non linear analysis (Fig 4, 5). Geometric modelling of children foot bone *in vivo* derived from MRI [HoBaTho et al. 1998] allowed to distinguish the osseous nucleus and cartilage anlage (Fig.6). The length of the foot is around 6cm. The models allowed to quantify the bone deformity and perform a preoperative planning surgery. Finite element models with individualised geometry and material properties *in vivo* of a vertebral body of two scoliotic patients (same age and sex). They both had a scoliotic deformity at the same level of the lumbar spine (L1). Figure 7 demonstrates clearly the individual difference in the geometry and material properties range and distribution [Périé et al. 2001].

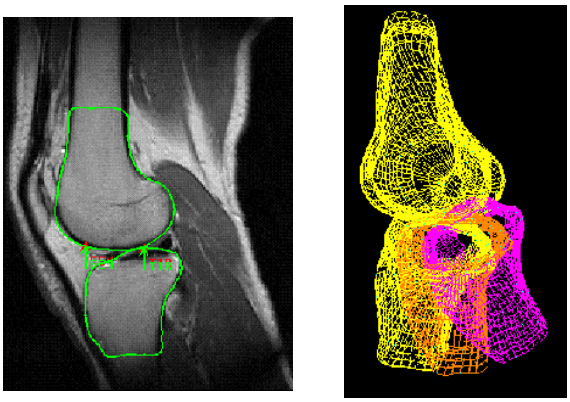

(a) (b)

Figure 4 : MRI of a knee in vivo (a) and geometrical reconstruction of the knee for different flexion (b).

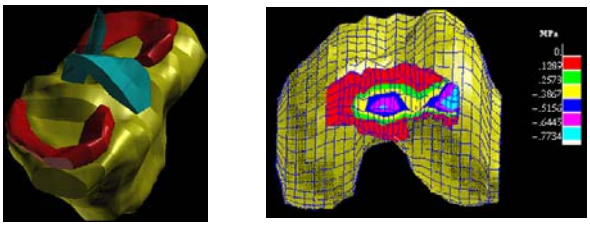

(a) (b)

Figure 5 : In vivo geometrical reconstruction of the anterior and posterior cruciate ligaments (blue) and meniscus (red) (a) and contact pressure visualised on the femoral condyles (b).

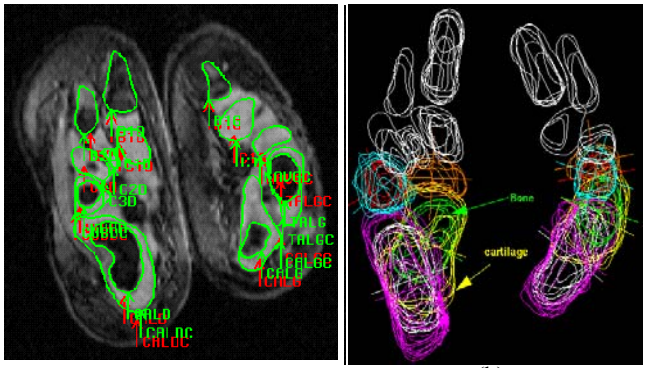

(a) (b)

Figure 6 : New born foot (a) and geometrical model (b)

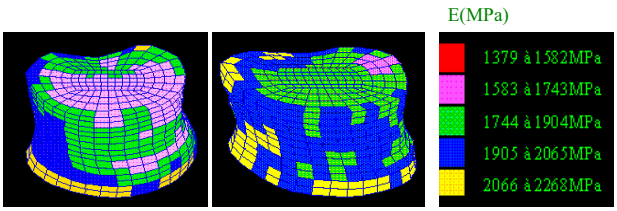

Figure 7 : Finite element models with individualised geometric and mechanical properties of scoliotic patient.

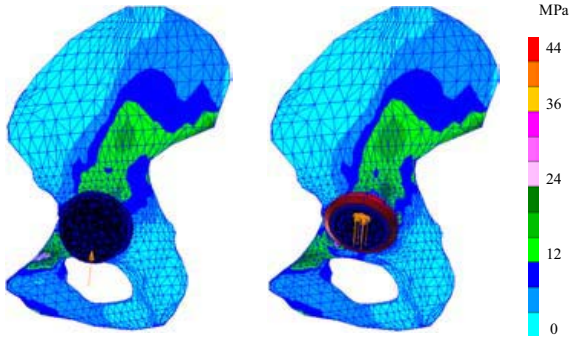

(a) (b)

Figure 8 : Von Mises Stresses for the model without implant (a) and with (b)

3.2 Examples of arthroplasty

Arthroplasty consisted in changing the damaged joint (hip, knee, shoulder) by artificial joints. Figure 8 illustrates numerical model of an acetabular implant of a patient before and after surgery (Hinrichs et al. 2001). In this study, significant influence of the assumptions on material properties have been demonstrated by assuming the material to be isotropic or anisotropic homogeneous, isotropic or anisotropic inhomogeneous.

It should be noted that Von Mises stress is not appropriate to predict risk of failure for anisotropic elastic properties such as bone. But it is often used for these materials to simplify the interpretation and to represent the six stress components in a generalized ‘stress intensity’ factor [Huiskes and Verdonschot 1997].

The methodology has been applied to design and evaluate a customized hip implant from medical images. The protocol consists in designing a customized implant by considering the geometrical and mechanical properties simultaneously of the patient data. In parallel, a 3D finite element model is developed to evaluate the design and predict its mechanical behavior in the patient’s femur [Barré 2000].

4 Discussion

4.1 Accuracy of the geometric modelling derived from medical images.

Accuracy of the geometric model depends on the technical protocol acquisition of the medical images and methodology used for processing them. The geometrical errors could be introduced by the spatial resolution of the image (pixel size is equal to the field of view divided by the matrix of pixels) and algorithm of edge detection and interpolation function.

A good spatial resolution allowed a better accuracy for the edge detection after the threshold process. Figure 9 a-b illustrates two different spatial resolution performed on the same image. The other source of error would be the choice of the values for the threshold process (Fig 9 b-c). For the same image with different values of thresholding may results different geometric results derived from curve interpolation. Increasing the spatial resolution will

Figure 9 : Geometric errors introduced by the spatial resolution (a compared to b) and the threshold process performed (b,c).

increase the patient dose irradiation for CT image, and time examination for MRI. In general, compromise has to be taken between the quality of the images and patient welfare. Acceptable range of spatial resolution would be less than 0.5mm (pixel value). It is clear that for each anatomical model sensitivity analysis has to be performed in order to define appropriate technical protocol of acquisition.

4.2 Models with individualised geometric and mechanical properties derived from medical images.

Quantitative measurements performed on the CT images required a good 'density' resolution. In order to achieve that, the technical protocol of acquisition of the images should be optimised. Influence of these parameters on direct measurements of CT number have been quantified and showed 10% of variation for the range of 0 to 1200 CT HU [HoBaTho et Treutenaere 2001]. This should be considered when predictive relationships are used to predict elastic properties from literature. The methodology of bone modelling with individualised geometric and mechanical properties needed to be improved for MRI data, as tissue characterization is not reflecting significantly the material properties. In fact, the grey level of the region of interest is related to the intensity of proton density, which varies significantly with the acquisition parameters. When predictive relationships are not appropriate, the atlas database is used. When needed, this database is increased with other bones using the transmission ultrasonic technique [Baréa et al. 1997].

4.3 Experimental validation

Before using our method in an *in vivo* case (patient case) our methodology has been validated in an *in vitro* case (cadaveric specimen) for customised hip implant [Couteau et al. 1998], tibial implant [Estivalèzes et al. 1999], glenoid implants [Baréa et al. 1999]. Then in vivo modelling could be assessed for testing and predicting the short and long term implant behaviour. The results can only be validated by the clinical follow up and evaluation on the patient.

5 Conclusions and perspectives

Relevance of such techniques is their direct clinical application for modelling patient specific bone and joints. This provides an individual diagnosis and preoperative planning surgery or orthopaedic treatment.

Technical protocol of image acquisitions is of importance in the methodology; spatial and density resolution have to be achieved to reduce geometric and material properties errors.

The methodology needs to be improved by :

- the investigation of assessment of material properties of soft tissue derived from MRI
- the investigation of automatic meshing technique dedicated to bone and joints anatomy; in order to reduce the time consuming in performing a finite element model of bone and joints.

These are challenging investigations for the next decade. From the results of in vivo modelling of bone and joints

obtained with these techniques, one would expect objective criterias for planning surgery or orthopaedic treatment and standardization for development of implants or orthoses.

Acknowledgement: The author would like to acknowledge Texas Scottish Rite Hospital for Children, Fondation pour la Recherche Médicale, INSERM (Institut National de la Santé et de la Recherche Médicale), CNRS (Centre National de la Recherche Scientifique) for their support. Clinicians from Orthopaedic Surgery and Radiology Departments of TSHR, CHU Purpan Toulouse and Polyclinique St Côme Compiègne are acknowledged for their scientific contribution.

Reference

Ashman, R.B.; Cowin, S.C.; Van Buskirk, W.C.; Rice, J.C. (1984): A continuous wave technique for the measurement of the elastic properties of cortical bone. *J. Biomech, 1984, Vol 17, 349-361.*

Ashman, R.B.; Rho, J.Y.; Turner, C.H. (1989): Anatomical variation of orthotropic elastic moduli of the proximal human tibia. *J Biomech,* Vol 22, pp 895-900.

Baréa, C.; Mansat, P.; HoBaTho, M.C.; Darmana, R.; Mansat, M. (1997): Mechanical properties of the cancellous bone of the glenoid. *Transactions of the Orthopaedic Research Society 877.*

Baréa, C.; HoBaTho, M.C.; Darmana, R.; Mansat, M. (1998) :3D finite element study of glenoid implants in total shoulder arthroplasty. In : J. Middleton, ML Jones, G Pande (eds) *Computer methods in Biomechanics and Biomedical* Engineering Gordon and Breach Science Publishers pp. 471-479.

Barré C. (2000) Mise en place d'une méthodologie pour la conception et l'évaluation d'une prothèse de hanche personnalisée. Master Sciences dissertation. UTC 2000.

Carter, D.R; Vasu, R.; Harris, W.H. (1984): Stress changes in the femoral head due to porous ingrowth surface replacement arthroplasty. *J Biomech,* Vol 17, pp 737-747.

Couteau, B.; HoBaTho, M.C.; Darmana, R.; Brignola, J.C.; Arlaud, J.Y. (1998): Development of a finite element model of a human femur with individualized geometry and mechanical properties: validation by vibration analysis. *Technical Note J Biomech* , vol. 31, pp. 383-386.

Couteau, B; Labey, L; HoBaTho M.C.; Vander Sloten, J; Arlaud, J.Y.; Brignola, J.C. (1998): Validation of a three dimensional finite element model of a human femur with a customized hip implant. In : J. Middleton, ML Jones, G Pande (eds) *Computer methods in Biomechanics and Biomedical* Engineering Gordon and Breach Science Publishers, pp. 147-154.

Estivalèzes, E.; Couteau, B.; Limbert, G.; Darmana, R.; HoBaTho, M.C. (1999): Etude du comportement mécanique d'un tibia sain et prothésé, modélisation par éléments finis et validation expérimentale. *Actes du 4ème colloque national en calcul des structures, vol. II, pp. 791-796.*

Fischer, K.J; Bastidas, J.A; Pfafelle, H.J; Towers, J.D. (2003): A method for estimating relative bone loads from CT data with application to the radius and ulna. *CMES: Computer Modeling in Engineering and Sciences*, vol. 4, no. 3&4, pp. 397-403.

Keyak, J.H.,; Meager, J.M.; Skinner, H.B.; Mote, C.D. (1990) : Automated three-dimensional finite element modelling of bone : a new method. *J Biomed Eng*, vol. 12, pp.389-397.

Keyak, J.H.,; Fourkas, M.G.; Meager, J.M.; Skinner, H.B. (1993) : Validation of an automated method of three dimensional finite element modelling of bone. *J Biomed Eng*, vol. 12, pp.389-397.

HoBaTho, M.C.; Darmana, R.; Pastor, P.; Barrau, J.J., Laroze, S., Morucci, J.P. (1991) : Development of a three-dimensional finite element model of a human tibia using experimental modal analysis. *J Biomech*, vol. 24, pp 371-383.

HoBaTho, M.C.; Rho, J.Y.; Ashman, R.B. (1992) : Atlas of mechanical properties of human cortical and cancellous bone. In : Van der Perre G., Lowet G. , Borgwardt A (eds) *In vivo assessment of bone quality by vibration and wave propagation techniques, Part II* , ACCO, Leuven, pp. 7-38.

HoBaTho, M.C. (1993) Logiciel SIP 305, Logiciel de prétraitement d'images médicales, Scanner, IRM.

HoBaTho, M.C.; Rho, J.Y.; Ashman, R.B. (1998): Anatomical variation of mechanical properties of human cancellous bone in vitro. In : G. Lowet, P. Rüegsegger, H. Weinans and A. Meunier (eds) *Bone Research in Biomechanics, IOS Press*, pp 157-173.

HoBaTho, M.C.; Luu, S.; Estivalèzes, E.; Baunin, C.; Cahuzac, J.P. (1998) : Simulation of the 3D motion

of clubfoot bones using helical axes theory. *Suppl. J Biomech, vol 31, pp. 107.*

HoBaTho, M.C.; Treutenaere J.M. (2001) : Influence of acquisition parameters on QCT measurements derived from CT. Proceedings XVIIIth Congress of the International Society of Biomechanics, Zurich, 2001 pp 102-103.

Hinrichs, M.; Luu, S.; Roux, F.; Treutenaere, J.M.; HoBaTho, M.C. (2001) : In vivo analysis of the pelvic bone before and after acetabular reconstruction by means of a three dimensional finite element model. Proceedings XVIIIth Congress of the International Society of Biomechanics, Zurich, 2001 pp 102.

Huiskes, R.; Chao, E.Y.S. (1983) : A survey of finite element analysis in orthopaedic biomechanics: the first decade. *J Biomech*, vol. 16, pp. 385-409.

Huiskes, R.; Verdonschot, N. (1997) : Biomechanics of artificial joints : the hip. In : V. C. Mow and W. Hayes (eds) *Basic Orthopaedic Biomechanics, pp. 395-460.*

Johnston, C.E.; HoBaTho, M.C.; Baker, K.J.; Baunin, C. (1995): Three dimensional analysis of clubfoot deformity using computed tomography. *J Pediatr Orthop*, vol. 4. Part B, pp. 39-48.

Limbert, G.; Estivalèzes, E.; HoBaTho, M.C.; Baunin C.; Cahuzac J.P. (1998): In vivo determination of homogenised mechanical characteristics of human tibia. Application to the study of tibial torsion in vivo. *Clin Biomech* , vol. 13, pp. 473-479

Périé, D.; HoBaTho, M.C. (1998) : In vivo determination of contact areas and pressure of the femorotibial joint using non linear element analysis. *Clin Biomech* , vol. 13, pp. 394-402.

Périé, D.; Sales De Gauzy, J.; Sévely, A.; HoBaTho, M.C. (2001): In vivo geometrical evaluation of Cheneau Toulouse Munster brace effect on scoliotic spine using MRI method. *Clin Biomech* , vol. 16, pp. 129-137

Périé, D.; Sales De Gauzy, J.; Baunin, C.; HoBaTho, M.C. (2001): Tomodensitometry measurements for in vivo quantification of mechanical properties of scoliotic vertebrae *Clin Biomech* , vol. 16, pp. 373-379.

Prendergast, P. (1997): Finite element models in tissue mechanics and orthopaedic implant design. Review paper. *Clin Biomech*, vol.12, pp. 343-366.

Rho, J.Y.; HoBaTho, M.C.; Ashman, R.B. (1995): Relations of mechanical properties to density and CT numbers in human bone. *Med Eng Phys*, vol. 17, (5), pp. 347-355.

Roach, J.W.; HoBaTho, M.C.; Baker, K.J.; Ashman, R.B. (1997) : Three-dimensional computer analysis of complex acetabular insufficiency. *J Pediatr Orthop*, vol.17, pp. 158-164.

Van der Sloten, J.; HoBaTho, M.C.; Verdonck, P. (1998): Applications of computer modelling for the design of orthopaedic, dental cardiovascular biomaterials. *Proc Instn Mech Engrs*, vol. 212, Part H, pp. 489-500.

Viceconti, M.; Zannoni, C., Baruffaldi, F; Pierotti, L.; Toni, A.; Cappello, A. (1998) : CT scan data acquisition to generate biomechanical models of bone structures. In : J. Middleton, ML Jones, G Pande (eds) *Computer methods in Biomechanics and Biomedical* Engineering Gordon and Breach Science Publishers pp. 279-287.